

CHEMISTRY

A European Journal

A Journal of



Accepted Article

Title: Selective Catalytic Performances of Noble Metal Nanoparticle@MOF Composites: the Concomitant Effect of Aperture Size and Structural Flexibility of MOF Matrices

Authors: Luning Chen, Wenwen Zhan, Huihuang Fang, Zhenmin Cao, Chaofan Yuan, Zhaoxiong Xie, Qin Kuang, and Lansun Zheng

This manuscript has been accepted after peer review and appears as an Accepted Article online prior to editing, proofing, and formal publication of the final Version of Record (VoR). This work is currently citable by using the Digital Object Identifier (DOI) given below. The VoR will be published online in Early View as soon as possible and may be different to this Accepted Article as a result of editing. Readers should obtain the VoR from the journal website shown below when it is published to ensure accuracy of information. The authors are responsible for the content of this Accepted Article.

To be cited as: *Chem. Eur. J.* 10.1002/chem.201702103

Link to VoR: <http://dx.doi.org/10.1002/chem.201702103>

Supported by
ACES

WILEY-VCH

Selective Catalytic Performances of Noble Metal Nanoparticle@MOF Composites: the Concomitant Effect of Aperture Size and Structural Flexibility of MOF Matrices

Luning Chen,^[a] Wenwen Zhan,^[b] Huihuang Fang,^[a] Zhenmin Cao,^[a] Chaofan Yuan,^[a] Zhaoxiong Xie,^[a] Qin Kuang,^{*[a]} and Lansun Zheng^[a]

Abstract: Noble metal nanoparticles embedded in metal organic frameworks (MOFs) are new composite catalysts with enhanced or novel properties compared to the pristine counterparts. In the past years, to determine the role of MOFs during catalytic process, most of studies focus on the confinement effect of MOFs, but ignore the structural flexibility of MOFs. In this paper, we use two composite catalysts, Pt@ZIF-8 [Zn(mIM)₂, mIM = 2-methyl imidazole] with flexible structure and Pt@ZIF-71 [Zn(DCIIM)₂, DCIIM = 4,5-dichloroimidazole] with rigid structure, and hydrogenation of cinnamaldehyde as model reaction, to show the confinement effect and the structure flexibility of MOF matrices on the catalytic performance of composite catalysts. Both catalysts showed high selectivity for cinnamic alcohol with the confinement effect of aperture. But, compared to Pt@ZIF-71, Pt@ZIF-8 exhibited higher conversion but lower selectivity owing to the flexible structure. The above results remind us that we will have to consider both the aperture size of MOFs and structure flexibility to select the proper MOF matrices for the composite materials to achieve the optimized performances.

Introduction

Noble metal nanoparticles (NPs) are high-efficiency catalysts for many chemical reactions due to their large surface area and abundant unsaturated coordinated atoms.^[1] Among noble metals, Pt has excellent catalytic activity for hydrogenation reactions with its superior "H-H" bond breaking capacity.^[2] However, just because of this high catalytic activity, Pt NPs have certain limitations in the chemoselective hydrogenation of the compounds with two and more double bonds, which is crucial for the production of commodity chemicals as well as fine and special chemicals.^[3] Consequently, it is highly desirable to explore Pt-based catalysts with high activity and selectivity for selective hydrogenation reactions.

Recently, composite materials with noble metal NPs (such as Pt, Pd, Au, and Ag) embedded in metal organic frameworks (MOFs) have attracted increasing attentions because they combine the tailorable porosity of MOFs with the versatile functionality of noble metal NPs, such as catalysis, sensing, and so on.^[4] For this kind of composite materials, the aggregation of noble metal NPs can be significantly prevented by the MOF matrices, thereby keeping the surface structure of noble metal NPs and its related effects well preserved. On the other hand, the regular and well-defined cavities of MOF matrices can provide confined microenvironment for the molecular diffusion/adsorption onto the NP surface, thereby accelerating reaction rates and/or changing reaction pathways.^[4c, 5, 6] Owing to the synergism effect between two functional materials, the noble metal NPs embedded in MOFs often exhibit enhanced or even novel properties compared to their pristine counterparts; therefore, they are hopefully endowed with high activity and good selectivity in heterogeneous catalytic reactions.^[7] Determining the role of MOF matrices in catalysis is one of the central issues for the successful application of such composite materials.^[8] In the past years, most of studies just focus on the confinement effect of MOF matrices due to their small apertures, but the influence from the structural flexibility of MOF matrices, which have been deeply studied in gas absorption/separation, are often ignored.^[9] However, the structural flexibility of MOFs likewise has a significant influence on the diffusion/adsorption of reaction molecules in MOF cavities.^[10] Consequently, flexible frameworks may weaken the size confinement effect during the catalytic process so as to produce some exceptional results compared to those composite catalyst with rigid MOFs as matrices.

Herein, we specifically synthesized two kinds of composite catalysts with Pt NPs embedded in MOF matrices, Pt@ZIF-8 and Pt@ZIF-71, to show the concomitant effect of the aperture size and the structure flexibility of MOF matrices on the catalytic performance of composite catalysts. The results demonstrate that the two composite catalysts were highly efficient to the selective hydrogenation of cinnamaldehyde (CAL) to cinnamic alcohol under mild conditions due to the confinement effect for the small apertures of MOF matrices. But the catalyst with Pt NP embedded in flexible matrices (i.e., Pt@ZIF-8) was found to be much higher in conversion but lower in selectivity than the catalyst with embedded in rigid matrices (i.e., Pt@ZIF-71) due to the flexible structure of ZIF-8 frameworks.

Results and Discussion

[a] L. Chen, H. Fang, Z. Cao, C. Yuan, Prof. Z. Xie, Prof. Q. Kuang, Prof. L. Zheng
State Key Laboratory for Physical Chemistry of Solid Surfaces
Collaborative Innovation Centre of Chemistry for Energy Materials
Department of Chemistry
College of Chemistry and Chemical Engineering
Xiamen University, Xiamen, 361005 (P.R. China)
E-mail: gkuang@xmu.edu.cn

[b] Dr. W. Zhan
Department of Chemistry
School of Chemistry and Chemical Engineering
Jiangsu Normal University, Xuzhou, 221116 (P.R. China)

Supporting information for this article is given via a link at the end of the document.



Scheme 1. The synthetic process of Pt NP embedded MOF composite catalysts and the crystallographic structures of corresponding ZIF-8 and ZIF-71 matrix.

The Pt@ZIF-8 and Pt@ZIF-71 composite catalysts were prepared according to a previously reported encapsulation method, in which the Pt NPs used need to be modified with a layer of PVP to improve the compatibility of Pt NP surfaces with organic ligands (Scheme 1).^[11] In both synthetic processes, the content of Pt NPs in the composite catalysts was tuned through adding different volumes of the pre-prepared methanol solution of PVP-modified Pt NPs (5 mg/mL) into the growth solutions of MOF matrices. For convenience, the as-prepared composite catalysts were denoted as Pt@ZIF-8-X% or Pt@ZIF-71-X% (X% = 1%, 3%, 5%, and 10%) according to the theoretical contents of Pt NPs. Structurally, ZIF-8 possesses a sodalite zeolitic-type structure featuring large cavities (11.6 Å) and small apertures (3.4 Å), and thus it only allows in principle for intrusion and diffusion of small molecules into the frameworks.^[12] As counterpart, ZIF-71 is a rigid MOF with a RHO topology and has larger cavities (16.8 Å) and pore apertures (4.8 Å).^[13] But recent studies have demonstrated that the sodalite cell of ZIF-8 can shrink or expand upon the pressure stimulus, thereby allowing the intrusion of larger molecules than the aperture size of ZIF-8 into cavities.^[14] Besides, it is also proposed that a short-lived “open” state happens to ZIF-8 due to the linker dissociation, which allows larger substrate molecules easily pass through the aperture of ZIF-8.^[15] Predictably, this unique flexible feature of ZIF-8 has a significant impact on the confinement effect of MOF matrices in the practical applications including catalysis.

The morphologies of blank MOF matrices (i.e., ZIF-8 and ZIF-71) and their composites with Pt NPs embedded were first revealed by scanning electron microscopy (SEM) (Figure S1). All the products, whether with Pt NPs embedded or not, are rhombic dodecahedra with uniform shape and size. This indicates that the crystallization habits of ZIF-8 or ZIF-71 cannot be changed by the introduction of Pt NPs. Compared to the microsized ZIF-71 series, the sizes of ZIF-8 series are only 300–400 nm. The transmission electron microscopy (TEM) images (Figure 1a, b) and associated elemental mappings (Figure S2, S3) further reveal that the most of Pt NPs are randomly embedded in ZIF-8 or ZIF-71 matrices, without obvious aggregation, and the embedding densities increase with the increase of feeding ratio of the Pt NPs. Accordingly, the colours of both two series are gradually deepened, changing from white to dark grey (Figure S4). Of particular note, high-magnification TEM images (Figure S5) clearly reveal that a few Pt NPs are embedded on the external surface of MOFs, especially in the cases of high Pt content (5% and 10%).

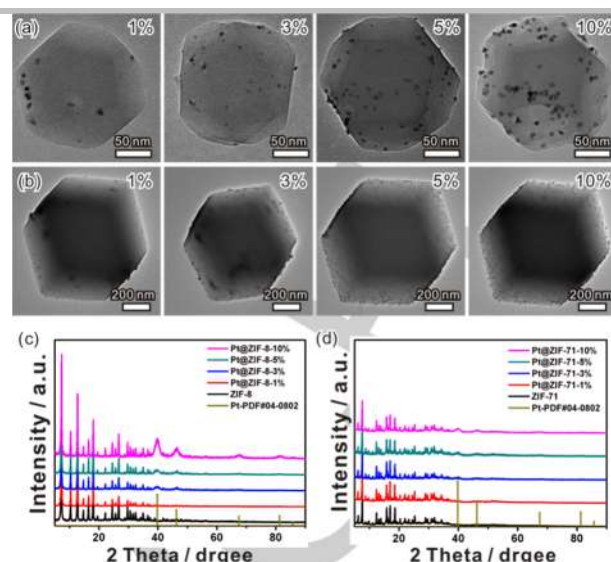
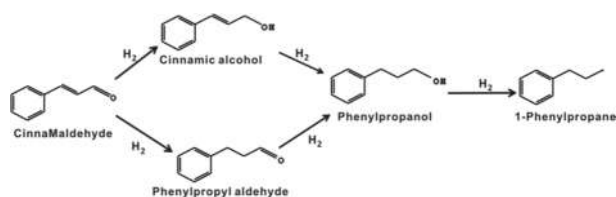


Figure 1. (a, b) TEM images and (c, d) their XRD patterns of Pt@ZIF-8-X% and Pt@ZIF-71-X% (X% = 1, 3, 5, 10%).

The composition of composite catalysts was examined by powder X-ray diffraction (XRD, Figure 1c, d). For Pt@ZIF-8-1% and Pt@ZIF-71-1%, the XRD patterns match well with the simulated pattern of ZIF-8 and ZIF-71, respectively, and no diffraction peaks assigned to Pt are detected due to the small size of Pt NPs and their low contents in the composites. When the theoretical Pt content is above 3%, some weak and broad diffraction peaks corresponding to the characteristic peaks of face-centered cubic Pt (JCPDS no. 04-0802) appear in the XRD pattern of composites together with the peaks assigned to ZIF-8 or ZIF-71. With the increase of Pt NPs added, these additional diffraction peaks become more and more prominent. According to the Debye-Scherrer formula, the calculated average sizes of Pt NP from the (111) diffraction peaks are ca. 4.5 nm, which is consistent with the TEM observed value (4.3 nm) of the original PVP-modified Pt NPs (Figure S6). The inductively coupled plasma mass spectrometry (ICP-MS) analysis indicates that the actual contents of Pt in the composites increase with the addition of PVP-modified Pt NPs in growth solution, but all are lower than their corresponding nominal values. This deviation is probably caused by the loss of unsuccessfully embedded Pt NPs in the washing treatment.

Nitrogen adsorption/desorption isotherms were measured to evaluate the influence of embedding of Pt NPs on the internal surface areas and pore size distributions of MOF matrices. The two series of composites both display type-I isotherms similar to the blank ZIF-8 or ZIF-71 matrices, in which the steep increase in N₂ uptake at a low relative pressure (<0.01) presents the characteristic of microporous materials (Figure S7). Of note, in contrast to the ZIF-71 series with larger size, the ZIF-8 series of 300–400 nm display an obvious N₂ uptake at high relative pressure, which indicates the existence of textural meso/macroporosity formed by packing of Pt@ZIF composite particles.^[16] And with increasing of Pt feeding, more PVP exists in the solution, which will somewhat influence the size and morphology of ZIF-8. Table S1 lists the calculated specific surface areas of the two series according to the Brunauer-Emmett-Teller (BET) model. Because of the smaller sizes, the surface areas of the ZIF-8 series (1060–1400 m²/g) are higher than those of the ZIF-71 series (720–820 m²/g). Compared with the pure ZIF-8 or ZIF-71, the composite catalysts with low Pt loading amounts possess higher specific surface areas (e.g.,

1402 m²/g for Pt@ZIF-8-1% and 821 m²/g for ZIF@ZIF-71-1%), owing to the presence of structure defects in the MOF matrices during the incorporation of Pt NPs. And with more Pt NPs embedded, the surface area of these composite catalysts consistently decrease, since more and more cavities of MOF matrices are blocked by Pt NPs.^[17]



Scheme 2. Schematic diagram of the cinnamaldehyde hydrogenation.

In this study, we chose cinnamaldehyde (CAL) as a model molecule, which is a common chain compound with a “C=C” bond and a “C=O” bond, to show how the aperture size and structural flexibility of MOFs influence the catalytic performance in chemoselective hydrogenation of α,β -unsaturated aldehydes.^[18] Principally, CAL can be converted to various hydrogenated products such as (a) cinnamic alcohol, (b) phenylpropyl aldehyde, (c) phenylpropanol, and (d) phenylpropane as illustrated in Scheme 2, of which, cinnamic alcohol is a common essence and medical intermediate to synthesize hypotensor and anti-carcinogen. However, the formation of saturated aldehydes for α,β -unsaturated aldehydes like CAL is thermodynamically favoured over the unsaturated alcohol. Therefore, the chemoselective hydrogenation of α,β -unsaturated aldehydes to the corresponding unsaturated alcohol remains a scientific challenge to date.^[19]

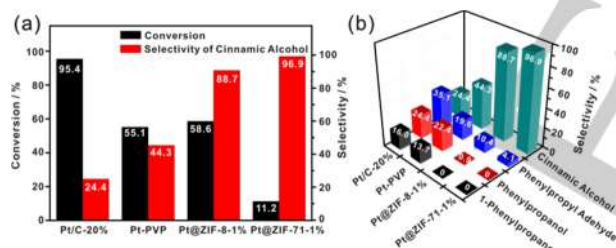


Figure 2. (a) Comparison of the conversions of CAL hydrogenation and the selectivities for cinnamic alcohol over Pt/C-20%, Pt-PVP, Pt@ZIF-8-1% and Pt@ZIF-71-1%. (b) Comparison of the selectivity for four products over four catalysts.

The results of CAL hydrogenation over the blank MOF matrices and their composites with different Pt loading amounts are listed in Table S2. And 20% carbon matrixed platinum (Pt/C-20%) and PVP-stabilized Pt NPs (Pt-PVP) were also tested as the reference catalysts. It should be stressed here that the Pt NPs embedded in all the composite catalysts added are normalized to the same weight (5 mg) in the tests according to their ICP-MS results. Over Pt/C-20%, the conversion of CAL was very high (95.4%), but all possible hydrogenation forms are produced, with only 24.4% selectivity for cinnamic alcohol. By contrast, the PVP-modified Pt NPs give higher cinnamic alcohol selectivity (44.3%) and lower conversion of CAL (55.1%), which is attributed to the steric effect of PVP on the adsorption of CAL molecules on the surface of Pt NPs.^[20] However, after Pt NPs are embedded in MOF matrices, the resulting composite catalysts show distinct catalytic performances from those unencapsulated Pt NPs. Take Pt@ZIF composites with loading amount of 1% for example. As

shown in Figure 2a, the selectivity of cinnamic alcohol over Pt@ZIF-8-1% and Pt@ZIF-71-1% is raised to 88.7% and 96.9%, respectively, although the conversion of CAL significantly decreases to 58.6% and 11.2%, respectively. Furthermore, the excessive hydrogenation of CAL is almost completely inhibited in the two Pt embedded cases (Figure 2b). However, the pure ZIF-8 and ZIF-71 without Pt NPs showed no activity, which indicates that organic links (mIM, DCIM), ZnN₄ tetrahedra, and their defective sites do not contribute to the catalytic reaction. It should be noted that all the composite catalysts possess very good structural and chemical stability during the catalysis tests (Figure S8, S9), and the size of Pt NPs can be well kept without agglomeration (Figure S10). Besides that, the ICP-MS analysis reveals that there is no loss of Pt NPs after catalysis (Table S3) which indirectly proves that most of Pt NPs are embedded in the MOF matrices.

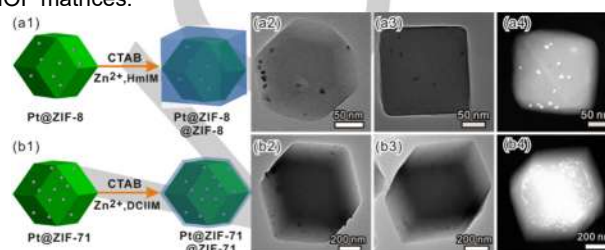


Figure 3. (a₁, b₁) The formation process of sandwich-structured Pt@ZIF@ZIF composites. (a₂, b₂) TEM images of Pt@ZIF-8-1% and Pt@ZIF-71-1%. (a₃, b₃) TEM images and (a₄, b₄) STEM images of Pt@ZIF-8-1% and Pt@ZIF-71-1% after encapsulated in the corresponding ZIFs.

As observed in TEM images, some Pt NPs fail to be embedded into the MOF matrices in the two series of Pt@ZIF composites with the amount of Pt loading increasing. Admittedly the presence of these unencapsulated Pt NPs may influence the determination of the intrinsic role of MOF matrices, because they exhibit distinct catalytic properties from those in the MOF matrices due to the lack of confined microenvironment. In order to exclude the effect of the unencapsulated Pt NPs located on the surface, two series of composites with a unique sandwich-like structure, Pt@ZIF-8@ZIF-8 and Pt@ZIF-71@ZIF-71, were specially synthesized in our study (Figure S11). As illustrated in Figure 3a₁ and 3b₂, another ZIF-8 or ZIF-71 shell epitaxially grows on the surface of the original Pt@ZIF catalysts with the assistance of cetyltrimethyl ammonium bromide (CTAB), leading to the formation of the sandwich-like structure.^[8a, 21] By comparison of the TEM and scanning transmission electron microscopy (STEM) images of the Pt@ZIFs before and after the second growth, it is clearly seen that all the Pt NPs have been absolutely encapsulated within MOF matrices in the sandwich-like structures (Figure a₂₋₄ and Figure b₂₋₄). Interestingly, after growing a ZIF shell, the morphologies of all Pt@ZIF-8 composite change from rhombic dodecahedra to cube due to the specific adsorption of CTAB on the ZIF-8 {100} faces.^[22] By contrast, the morphologies of all the as-formed Pt@ZIF-71@ZIF-71 still keep rhombic dodecahedral, the same as Pt@ZIF-71. The nitrogen adsorption/desorption isotherms of the sandwich-structured samples is similar to the original Pt@ZIF samples (Figure S12). The surface areas of ZIF-8 series (1000–1200 m²/g) are higher than ZIF-71 series (700–800 m²/g) like the original composites (Table S4). The ICP-MS analysis reveals that the actual Pt contents in the sandwich-structured samples almost remain the same with the values in the original Pt@ZIF samples, which shows that Pt NPs embedded on the external surface of MOF matrices didn't fall off during the growth of ZIF outer shells.

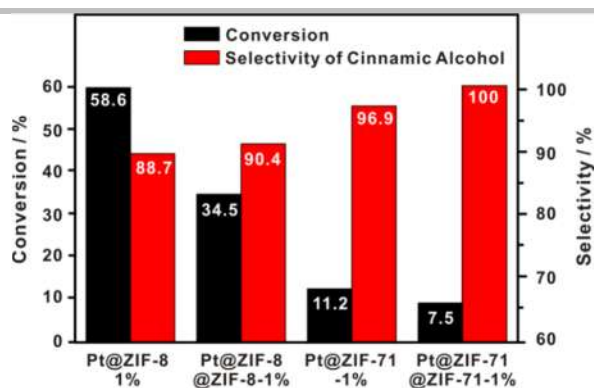


Figure 4. Comparison of the conversions of CAL hydrogenation and the selectivities for cinnamic alcohol over Pt@ZIF-8-1%, Pt@ZIF-71-1%, and Pt@ZIF-8-1%, Pt@ZIF-71-1% embedded in corresponding ZIF shell.

Considering that the effect of the unencapsulated Pt NPs has been excluded in the as-synthesized sandwich-like structures, we further investigated their catalytic performances in the CAL hydrogenation reaction (Table S5). In comparison with the original Pt@ZIF catalysts, the conversion of CAL over the two series of sandwich-structured Pt@ZIF@ZIF catalysts significantly decreases, but the selectivity of cinnamic alcohol is raised to some extent. Taking Pt@ZIF-8-1% and Pt@ZIF-71-1% as examples, the performances of the catalysts before and after growing the ZIF shell are directly compared in Figure 4. The conversion of CAL over Pt@ZIF-8@ZIF-8-1% and Pt@ZIF-71@ZIF-71-1% is reduced to 34.5% and 7.5% from 58.6% and 11.2%, respectively, while the selectivity of cinnamic alcohol is raised to 90.4% and nearly 100% from 88.7% and 96.9%, respectively (Figure 4). Clearly, these changes are caused by the sandwich-structure that confirms there are no Pt NPs exposed on the surface of ZIFs. This result indicates that the outer ZIF shell not only depresses the diffusion of CAL onto the Pt NPs, but also provides a completely confined microenvironment for the Pt NPs. Of particular note, the Pt@ZIF-8@ZIF-8 catalysts always exhibit higher conversion of CAL and lower selectivity of cinnamic alcohol than the Pt@ZIF-71@ZIF-71 catalysts, which well agrees with the results in the cases of Pt@ZIF catalysts. The same law for the catalytic performances of these composites was further confirmed by the time-dependent catalytic experiments. As shown in Figure 5a, the conversion of CAL over all the measured catalysts gradually increases with the extended reaction time at the initial stage, and reaches a plateau after 6 hours due to the state of chemical equilibrium. By contrast, the selectivity of cinnamic alcohol over the catalysts basically remain unchanged during the whole catalytic process (Figure 5b). However, no matter the reaction time, the Pt@ZIF-8@ZIF-8 exhibit higher conversion of CAL and lower selectivity of cinnamic alcohol compared to the Pt@ZIF-71@ZIF-71. When the above results are combined together, we could reasonably conclude that the catalytic performance differences of the composites with Pt NPs embedded in different MOFs are intrinsically caused by the structural differences of MOFs.

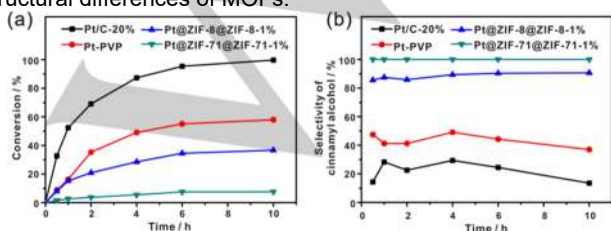


Figure 5. (a) The conversion of CAL and (b) the selectivity of cinnamic alcohol over different catalysts (Pt/C-20%, Pt-PVP, Pt@ZIF-8@ZIF-8-1% and Pt@ZIF-71@ZIF-71-1%) at different times.

It is widely acknowledged that the diffusion/absorption of guest molecules in MOFs is greatly confined to the sizes of apertures and cavities of MOFs, which usually leads to the decreased conversion of reactants. In view of small aperture sizes of ZIF-8 and ZIF-71, the CAL molecule with a benzene ring prefers to vertically adsorb on the Pt surface with aldehyde groups ("C=O"). Consequently, the H atoms produced due to the "H-H" bond breaking on the Pt surface would be selectively added into the "C=O" instead of "C=C", thereby improving the selectivity of cinnamic alcohol in the products.^[20, 23] However, in terms of this confinement effect of MOF matrices, there is a distinct difference between ZIF-8 and ZIF-71. Compared with Pt@ZIF-71 catalysts Pt@ZIF-8 catalysts show higher conversion but lower selectivity for cinnamic alcohol. Typically, the conversion of Pt@ZIF-8-1% (55.1%) is five times of Pt@ZIF-71-1% (11.2%), while the selectivity (88.7%) of the former is lower than that (96.9%) of the latter. This result is not normal, since ZIF-8 is supposed to display a stronger confinement effect in the catalytic conversion of CA due to its smaller apertures than ZIF-71. Clearly, there are other factors that significantly influence the confinement role of MOF matrices in the catalysis reaction.

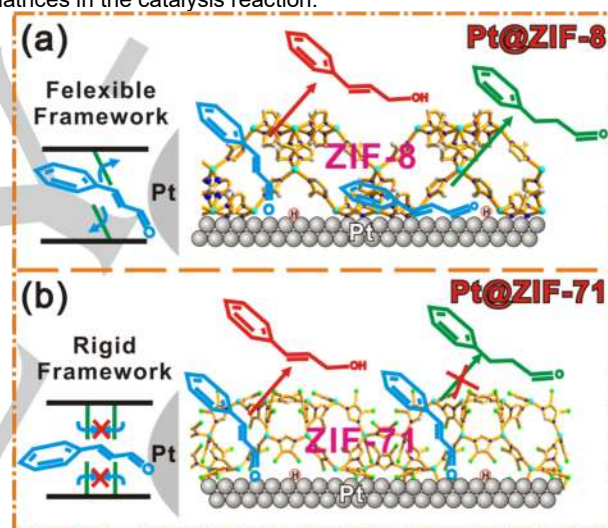


Figure 6. Schematic illustration for the hydrogenation of CAL on the Pt NP embedded within (a) flexible ZIF-8 and (b) rigid ZIF-71, respectively.

ZIF-8 is structurally a flexible structure due to the swinging of the $-CH_3$ groups and imidazolate linkers and dissociation of 2-methylimidazole to form the short-lived "open" states without disrupting the underlying MOF crystal structure and morphology, but ZIF-71 has no similar structural deformation.^[14, 15] This flexible feature of ZIF-8 makes CAL molecules more easily pass through the MOF pores and contact Pt NPs compared to in the case of ZIF-71, thereby leading to a higher conversion of Pt@ZIF-8 (Figure 6). After passing through ZIF-8's pores, CAL molecules have the possibility to adsorb on the Pt NPs flatly, which makes "C=C" bonds interact with the Pt surface and be hydrogenated, and therefore more by-products (phenylpropyl aldehyde, 9.6%) are produced for Pt@ZIF-8. No doubt, the abnormal catalytic performances of Pt@ZIF-8 catalyst should result from the structural deformation of flexible ZIF-8, which to some extent weakens the size confinement effect of MOF matrices.

Conclusions

In summary, two kinds of Pt embedded in MOF composite catalysts, Pt@ZIF-8 and Pt@ZIF-71, were specifically synthesized by the encapsulation method. The results revealed that the two composite catalysts were highly efficient to the selective hydrogenation of CAL to cinnamic alcohol under mild conditions due to the confinement effect from small apertures of MOFs matrices. But the Pt@ZIF-8 catalysts were found to exhibit higher catalytic efficiency and lower selectivity than Pt@ZIF-71, although ZIF-8 is smaller in the aperture size than ZIF-71. This is the first time to demonstrate that the structure flexibility of MOF matrices does make a significant influence on the confinement effect of MOF matrices, thereby leading to some exceptional catalytic performances of composite catalysts. Our present study provides some important insights into the structure-performance relationship of NP@MOF composites from a new perspective, which will help us to construct the composite materials with desired performances.

Experimental Section

Sample synthesis:

Synthesis of 3-5 nm PVP-modified Pt nanoparticles: the PVP-modified Pt NPs were prepared by refluxing a mixture of 533 mg PVP, aqueous solution of H_2PtCl_6 (15 mL, 8 mM), and methanol (180 mL) in a flask (500 mL) for 3 hours under air. And then methanol was removed by using rotary evaporator and the Pt NPs were cleaned with acetone and hexane to remove excess free PVP. After dried up, Pt NPs were finally dispersed in methanol to give a solution with Pt concentration of 5 mg / mL.

Synthesis of Pt@ZIF-8 and Pt@ZIF-71 composites: To make Pt NPs embedded in ZIF-8 matrices, a 1.38 mL pre-prepared methanol solution of Pt NPs was added into a 40 mL aqueous solution containing 5.5 g (67.1 mmol) 2-methylimidazole. After ultrasonic dispersion, a 3.0 mL $\text{Zn}(\text{NO}_3)_2$ methanol solution (0.5 mol/L) was added and the resulting solution was stirred for 6 hours under room temperature. Finally, the Pt@ZIF-8 catalyst was collected by centrifugation, followed by washing with ethanol several times and drying in the vacuum oven. In this case, the theoretical loading amount of Pt in the composite was 1 wt%, and the resulting composite catalyst was denoted as Pt@ZIF-8-1%.

In the synthesis of Pt@ZIF-71 with 1 wt% Pt loading (i.e., Pt@ZIF-71-1%), a 0.134 mL prepared methanol solution of Pt NPs was added into a 15 mL methanol solution containing 0.1046 g (0.76 mmol) 4,5-dichloroimidazole. After ultrasonic dispersion, a 15 mL zinc acetate (0.2 mmol) methanol solution was added into the above solution. After standing for 24 hours under room temperature, the Pt@ZIF-71-1% was collected by centrifugation, washed with ethanol several times, and dried in the vacuum oven. In both synthetic processes, the Pt loading amounts were tuned through adding different volumes of methanol solution of Pt NPs, and the resulting composite catalysts were denoted as Pt@ZIF-8-X% or Pt@ZIF-71-X% (X% =1%, 3%, 5%, 10%) according to the theoretical loading amounts of Pt NPs.

Synthesis of Pt@ZIF-8@ZIF-8 and Pt@ZIF-71@ZIF-71 composites: For epitaxially growing a ZIF-8 shell on the surface, 50 mg prepared Pt@ZIF-8 particles as seeds were dispersed in a solution prepared by mixing 5 mL deionized water and 750 μL 0.01 mol/L CTAB aqueous solution. And then 5 mL 1.32 mol/L HmlM aqueous solution mixed with 750 μL 0.01 mol/L CTAB aqueous solution was added into the Pt@ZIF-8 solution. After ultrasounding for five minutes, 5 mL 48 mmol/L $\text{Zn}(\text{NO}_3)_2$ aqueous solution was added into the solution. After ultrasound for

another five minutes, the resulting solution was stirred for 5 hours under room temperature. Finally, the as-formed Pt@ZIF-8@ZIF-8 catalyst was collected by centrifugation, followed by washing with ethanol several times and drying in the vacuum oven. The resulting composite catalysts were denoted as Pt@ZIF-8@ZIF-8-X% (X% =1%, 3%, 5%, 10%) according to the Pt@ZIF-8-X% dispersed.

As for Pt@ZIF-71@ZIF-71, the synthetic process was the same as Pt@ZIF-8@ZIF-8, except that methanol was used as solvent, 4,5-dichloroimidazole as organic linkers and zinc acetate as zinc sources.

Catalysis test: The catalysts, which contained about 5 mg Pt (0.5% molar ratio), were dispersed in 10 mL n-butyl alcohol, and then transferred into a pressure vessel. 0.4 mL cinnamaldehyde was added into the above solution. The vessel was flushed with H_2 flow for several minutes to remove the oxygen, and the pressurized to 3 atm. After reaction at room temperature for 6 h the solution was analyzed by gas chromatography-mass spectrometry (GC-MS, QP2010 Plus).

Acknowledgements

This work was supported by the National Basic Research Program of China (2015CB932301), the National Natural Science Foundation of China (2171163 and 21333008) and the Fundamental Research Funds for the Central Universities (20720160026). C. Yuan is grateful for the support of NFFTBS (No. J1310024).

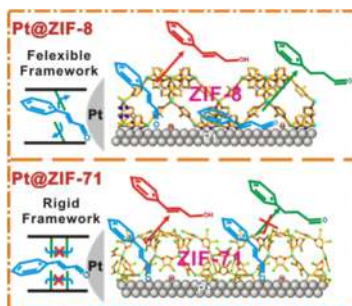
Keywords: metal-organic framework • composite catalyst • heterogeneous catalysis • structural flexibility • selective hydrogenation

- [1] E. Roduner, *Chem. Soc. Rev.*, **2006**, *35*, 583-592.
- [2] a) F. Zaera, *Chem. Rev.*, **1995**, *95*, 2651-2693; b) I. Lee, F. Delbecq, F. Morales, M. A. Albiter, F. Zaera, *Nat. Mater.*, **2009**, *8*, 132-138; c) P. E. Cremer, X. C. Su, Y. R. Shen, G. A. Somorjai, *J. Am. Chem. Soc.*, **1991**, *118*, 2942-2949; d) C. K. Tsung, J. N. Kuhn, W. Huang, C. Aliaga, L. Hung, G. A. Somorjai, P. Yang, *J. Am. Chem. Soc.*, **2009**, *131*, 5816-5822.
- [3] a) A. Corma, P. Serna, *Science*, **2006**, *313*, 332-334; b) M. Cargnello, V. Doan-Nguyen, T. R. Gordon, R. E. Diaz, E. A. Stach, R. J. Gorte, F. Fornasiero, C. B. Murray, *Science*, **2013**, *341*, 771-773; c) G. Chen, C. Xu, X. Huang, J. Ye, L. Gu, G. Li, Z. Tang, B. Wu, H. Yang, Z. Zhao, Z. Zhou, G. Fu, N. Zheng, *Nat. Mater.*, **2016**, *15*, 564-569.
- [4] a) N. Stock, S. Biswas, *Chem. Rev.*, **2012**, *112*, 933-969; b) I. Bradshaw, A. Garai, J. Huo, *Chem. Soc. Rev.*, **2012**, *41*, 2344-2381; c) Q. L. Zhu, Q. Xu, *Chem. Soc. Rev.*, **2014**, *43*, 5468-5512; d) C. M. Doherty, D. Buso, A. J. Hill, S. Furukawa, S. Kitagawa, P. Falcaro, *Acc. Chem. Res.*, **2014**, *47*, 396-405; e) W. W. Zhan, Q. Kuang, J. Z. Zhou, Y. J. Kong, Z. X. Xie, L. S. Zheng, *J. Am. Chem. Soc.*, **2013**, *135*, 1926-1933.
- [5] a) J. Liu, L. Chen, H. Cui, J. Zhang, L. Zhang, C. Y. Su, *Chem. Soc. Rev.*, **2014**, *43*, 6011-6061; b) Y. B. Huang, J. Liang, X. S. Wang, R. Cao, *Chem. Soc. Rev.*, **2017**, *46*, 126-157.
- [6] a) B. Yuan, Y. Pan, Y. Li, B. Yin, H. Jiang, *Angew. Chem.*, **2010**, *122*, 4148-4152; *Angew. Chem. Int. Ed.*, **2010**, *49*, 4054-4058; b) J. Yang, F. Zhang, H. Lu, X. Hong, H. Jiang, Y. Wu, Y. Li, *Angew. Chem.*, **2015**, *127*, 11039-11043; *Angew. Chem. Int. Ed.*, **2015**, *54*, 10889-10893; c) Q. Yang, Q. Xu, S. H. Yu, H. L. Jiang, *Angew. Chem. Int. Ed.*, **2016**, *55*, 3685-3689; d) C. H. Kuo, Y. Tang, L. Y. Chou, B. T. Sneed, C. N. Brodsky, Z. Zhao, C. K. Tsung, *J. Am. Chem. Soc.*, **2012**, *134*, 14345-14348; e) A. Aijaz, A. Karkamkar, Y. J. Choi, N. Tsumori, E. Ronnebro, T. Autrey, H. Shioyama, Q. Xu, *J. Am. Chem. Soc.*, **2012**, *134*, 13926-13929; f) S. Proch, J. Herrmannsdorfer, R. Kempe, C. Kern, A. Jess, L. Seyfarth, J. Senker, *Chem. Eur. J.*, **2008**, *14*, 8204-8212.

- [7] a) H. L. Jiang, T. Akita, T. Ishida, M. Haruta, Q. Xu, *J. Am. Chem. Soc.*, **2011**, *133*, 1304-1306; b) H. Liu, L. Chang, C. Bai, L. Chen, R. Luque, Y. Li, *Angew. Chem.*, **2015**, *128*, 5103-5107; *Angew. Chem. Int. Ed.*, **2016**, *55*, 5019-5023; c) W. Zhang, L. Wang, K. Wang, M. U. Khan, M. Wang, H. Li, J. Zeng, *Small* **2017**, *13*, 1602583-1602587; d) L. Chen, H. Li, W. Zhan, Z. Cao, J. Chen, Q. Jiang, Y. Jiang, Z. Xie, Q. Kuang, L. Zheng, *ACS Appl. Mater. Inter.*, **2016**, *8*, 31059-31066; e) F. Carson, S. Agrawal, M. Gustafsson, A. Bartoszewicz, F. Moraga, X. Zou, B. Martin-Matute, *Chem. Eur. J.*, **2012**, *18*, 15337-15344; f) V. Pascanu, F. Carson, M. V. Solano, J. Su, X. Zou, M. J. Johansson, B. Martin-Matute, *Chem. Eur. J.*, **2016**, *22*, 3729-3737.
- [8] a) M. Zhao, K. Yuan, Y. Wang, G. Li, J. Guo, L. Gu, W. Hu, H. Zhao, Z. Tang, *Nature*, **2016**, *539*, 76-80; b) Z. Li, R. Yu, J. Huang, Y. Shi, D. Zhang, X. Zhong, D. Wang, Y. Wu, Y. Li, *Nat. Commun.*, **2015**, *6*, 8248; c) Y. Liu, S. Liu, D. He, N. Li, Y. Ji, Z. Zheng, F. Luo, S. Liu, Z. Shi, C. Hu, *J. Am. Chem. Soc.*, **2015**, *137*, 12697-12703; d) G. Huang, Q. Yang, Q. Xu, S. H. Yu, H. L. Jiang, *Angew. Chem.*, **2016**, *128*, 7505-7509; *Angew. Chem. Int. Ed.*, **2016**, *55*, 7379-7383; e) B. Rungtaweeworani, J. Baek, J. R. Araujo, B. S. Archanjo, K. M. Choi, O. M. Yaghi, G. A. Somorjai, *Nano Lett.*, **2016**, *16*, 7645-7649; f) F. Carson, V. Pascanu, A. Bermejo Gomez, Y. Zhang, A. E. Platero-Prats, X. Zou, B. Martin-Matute, *Chem. Eur. J.*, **2015**, *21*, 10896-10902.
- [9] a) A. Schneemann, V. Bon, I. Schwedler, I. Senkovska, S. Kaskel, R. A. Fischer, *Chem. Soc. Rev.*, **2014**, *43*, 6062-6096; b) Y. Sakata, S. Furukawa, M. Kondo, K. Hirai, N. Horike, Y. Takashima, H. Uehara, N. Louvain, M. Meilikhov, T. Tsuruoka, S. Isoda, W. Kosaka, O. Sakata, S. Kitagawa, *Science*, **2013**, *339*, 193-196; c) M. D. Allendorf, R. J. T. Houk, L. Andruszkiewicz, A. A. Talin, J. Pikarsky, A. Choudhury, K. A. Gall, P. J. Hesketh, *J. Am. Chem. Soc.*, **2008**, *130*, 14404-14405; d) L. Hamon, P. L. Llewellyn, T. Devic, A. Ghoufi, G. Clet, V. Guillemin, G. D. Pirngruber, G. Maurin, C. Serre, G. Driver, W. van Beek, E. Jolimaite, A. Vimont, M. Daturi, G. Ferey, *J. Am. Chem. Soc.*, **2009**, *131*, 17490-17499; e) C. X. Chen, Z. Wei, J. J. Jiang, Y. Z. Fan, S. P. Zheng, C. C. Cao, Y. H. Li, D. Fenske, C. Y. Su, *Angew. Chem.*, **2016**, *128*, 10086-10090; *Angew. Chem. Int. Ed.*, **2016**, *55*, 9932-9936.
- [10] a) S. Yuan, L. F. Zou, H. X. Li, Y. P. Chen, J. S. Qin, Q. Zhang, W. G. Lu, M. B. Hall, H. C. Zhou, *Angew. Chem.*, **2016**, *128*, 10934-10938; *Angew. Chem. Int. Ed.*, **2016**, *55*, 10776-10780; b) W. Zhan, Y. He, J. Guo, L. Chen, X. Kong, H. Zhao, Q. Kuang, Z. Xie, L. Zheng, *Nanoscale*, **2016**, *8*, 13181-13185.
- [11] G. Lu, S. Li, Z. Guo, O. K. Farha, B. G. Hauser, X. Qi, Y. Wang, X. Wang, S. Han, X. Liu, J. S. DuChene, H. Zhang, Q. Zhang, X. Chen, J. Ma, S. C. Loo, W. D. Wei, Y. Yang, J. T. Hupp and F. Huo, *Nat. Chem.*, **2012**, *4*, 310-316.
- [12] K. S. Park, Z. Ni, A. P. Cote, J. Y. Choi, R. Huang, F. J. Uribe-Romo, H. K. Chae, M. O'Keeffe and O. M. Yaghi, *Proc. Natl. Acad. Sci.*, **2006**, *103*, 10186-10191.
- [13] W. Morris, B. Leung, H. Furukawa, O. K. Yaghi, N. He, H. Hayashi, Y. Houndonougbo, M. Asta, B. B. Laird and O. M. Yaghi, *J. Am. Chem. Soc.*, **2010**, *132*, 11006-11008.
- [14] a) D. Fairen-Jimenez, S. A. Moggach, M. T. Wharmby, P. A. Wright, S. Parsons, T. Duren, *J. Am. Chem. Soc.*, **2011**, *133*, 8900-8902; b) L. Zhang, Z. Hu, J. Jiang, *J. Am. Chem. Soc.*, **2013**, *135*, 3722-3728; c) S. A. Moggach, T. D. Bennett, A. K. Cheetham, *Angew. Chem.*, **2009**, *121*, 7221-7223; *Angew. Chem. Int. Ed.*, **2009**, *48*, 7087-7089; d) L. Zhang, G. Wu, J. Jiang, *J. Phys. Chem. C*, **2014**, *118*, 8788-8794.
- [15] a) O. Karagiari, M. B. Lalonde, W. Bury, A. A. Sarjeant, O. K. Farha, J. T. Hupp, *J. Am. Chem. Soc.*, **2012**, *134*, 18790-18796; b) J. V. Morabito, L. Y. Chou, Z. Li, C. M. Manna, C. A. Petroff, R. J. Kyada, J. M. Palomba, J. A. Byers, C. K. Tsung, *J. Am. Chem. Soc.*, **2014**, *136*, 12540-12543.
- [16] a) Y. Pan, Y. Liu, G. Zeng, L. Zhao and Z. Lai, *Chem. Commun.*, **2017**, 2071-2073; b) S. Ding, Q. Yan, H. Jiang, Z. Zhong, R. Chen and W. Xing, *Chem. Eng. J.*, **2016**, *296*, 146-153.
- [17] a) Y. Huang, Y. Zhang, X. Chen, D. Wu, Z. Yi and R. Cao, *Chem Commun.*, **2014**, *50*, 10115-10117; b) J. Juan-Alcañiz, J. Gascon and F. Kapteijn, *J. Mater. Chem.*, **2012**, *22*, 10102-10118.
- [18] a) L. Chen, H. Chen, Y. Li, *Chem. Commun.*, **2014**, *50*, 14752-14755; b) A. Nagendiran, V. Pascanu, A. Bermejo Gomez, G. Gonzalez Miera, C. W. Tai, O. Verho, B. Martin-Matute, J. E. Backvall, *Chem. Eur. J.*, **2011**, *22*, 7184-7189.
- [19] a) P. Mäki-Arvela, J. Hájek, T. Salmi, D. Y. Murzin, *Appl. Catal. A*, **2001**, *292*, 1-49; b) P. Gallezot, D. Richard, *Catal. Rev. Sci. Eng.*, **1998**, *40*, 81-126; c) C. J. Kliewer, M. Bieri, G. A. Somorjai, *J. Am. Chem. Soc.*, **2005**, *127*, 9958-9966; d) M. S. Ide, B. Hao, M. Neurock, R. J. Davis, *ACS Catal.*, **2012**, *2*, 671-683; e) G. Kennedy, L. R. Baker, G. A. Somorjai, *Angew. Chem.*, **2014**, *126*, 3473-3476; *Angew. Chem. Int. Ed.*, **2014**, *53*, 3405-3408.
- [20] B. Wu, H. Huang, J. Yang, N. Zheng and G. Fu, *Angew. Chem.*, **2011**, *124*, 3496-3499; *Angew. Chem. Int. Ed.*, **2012**, *51*, 3440-3443.
- [21] J. Zhuang, L. Y. Chou, B. T. Sneed, Y. Cao, P. Hu, L. Feng, C. K. Tsung, *Small*, **2015**, *11*, 5551-5555.
- [22] P. Hu, J. Zhuang, L. Y. Chou, H. K. Lee, X. Y. Ling, Y. C. Chuang, C. K. Tsung, *J. Am. Chem. Soc.*, **2014**, *136*, 10561-10564.
- [23] a) Z. Guo, C. Xiao, R. V. Maligal-Ganesh, L. Zhou, T. W. Goh, X. Li, F. Tesfagaber, A. Thiel, W. Huang, *ACS Catal.*, **2014**, *4*, 1340-1348; b) F. Liu, L. Chang, L. Chen, Y. Li, *ChemCatChem*, **2016**, *8*, 946-951.

FULL PAPER

Two composite catalysts (i.e. Pt@ZIF-8 and Pt@ZIF-71) were designedly synthesized to investigate the concomitant effect of aperture size and structural flexibility of metal-organic framework matrices in the catalysis application. Compared to the Pt NPs sheathed with the rigid MOFs (Pt@ZIF-71), Pt@ZIF-8 composite catalyst was found to exhibit higher conversion but lower selectivity owing to the flexible structure of ZIF-8 matrices.



Luning Chen, Wenwen Zhan, Huihuang Fang, Zhenmin Cao, Chaofan Yuan, Zhaoxiang Xie, Qin Kuang,* and Lansun Zheng

Page No. – Page No.
Selective Catalytic Performances of Noble Metal Nanoparticle@MOF Composites: the Concomitant Effect of Aperture Size and Structural Flexibility of MOF Matrices

Accepted Manuscript